Syntheses, Crystal Structures and Properties of Mn(II) and Co(II) Coordination Complexes Based on 1,10-Phenanthroline Derivative①

ZHANG Hua[a, b, c] JI Liu-Qing[c] SONG Yu-Zhu[c]
KONG Zhi-Guo[a, b, c] LI Cong[a, b, c] WANG Xiu-Yan[a, b, c②]

[a] (*Key Laboratory of Preparation and Applications of Environmental Friendly Materials, Jilin Normal University, Ministry of Education, Changchun* 130103, *China*)

[b] (*Key Laboratory of Functional Materials Physics and Chemistry of the Ministry of Education, Jilin Normal University, Ministry of Education, Changchun* 130103, *China*)

[c] (*Department of Chemistry, Jilin Normal University, Siping* 136000, *China*)

ABSTRACT Two new coordination complexes [Mn(L)$_2$(DNSA)] (**1**) and [Co(L)(1,4-bdc)]$_n$ (**2**) have been achieved under hydrothermal conditions (H_2DNSA = 3,5-dinitro-salicylic acid, 1,4-bdc = 1,4-benzenedicarboxylic acid and L = 2-(2-fluoro-6-fluorophenyl)-1*H*-imidazo[4,5-*f*][1,10]phenanthroline). **1** crystallizes in monoclinic, space group $P2_1/c$ with a = 15.871(3), b = 17.274(4), c = 16.078(3) Å, β = 113.03(3)°, V = 4056.6(16) Å^3, Z = 4, $C_{45}H_{22}Cl_2F_2MnN_{10}O_7$, M_r = 978.57, D_c = 1.602 g/cm^3, F(000) = 1980, μ(Mo*Ka*) = 0.536 mm^{-1}, R = 0.0437 and wR = 0.1065. **2** belongs to the monoclinic system, space group $C2/c$ with a = 14.665(2), b = 30.856(4), c = 11.237(2) Å, β = 111.166(2)°, V = 4742.0(12) Å^3, Z = 8, $C_{27}H_{14}ClCoFN_4O_4$, M_r = 517.80, D_c = 1.602 g/cm^3, F(000) = 2312, μ(Mo*Ka*) = 0.889 mm^{-1}, R = 0.0364 and wR = 0.0862. The central Mn(II) ion in **1** is six-coordinated by four nitrogen atoms from two L ligands and two oxygen atoms from one DNSA anion. In **2**, the two kinds of 1,4-bdc ligands link neighboring Co(II) atoms to yield a two-dimensional layer structure. The luminescence of **1** has been studied in detail. Moreover, thermal behaviors of **1** and **2** are also investigated.

Keywords: crystal structure, coordination complex, 1,10-phenanthroline derivative, thermal behavior;
DOI: 10.14102/j.cnki.0254–5861.2011–2901

1 INTRODUCTION

Recently, the design and synthesis of new coordination complexes are currently attracting considerable attention due to their potential applications as functional materials[1-4]. It is well known that novel complexes can be specially designed under hydrothermal conditions by the selection of metal ions with preferred coordination geometries, in consideration of the structures of organic ligands and the effects of reaction conditions[5-7]. Therefore, great quantities of coordination complexes with fascinating topological structures and properties have been synthesized and reported so far[8-11]. As we know, covalent bonds and noncovalent intermolecular forces can be used to construct various supramolecular architectures[12]. Recent study indicates that 1,10-phenanthroline derivatives have been widely used to construct supramolecular architectures not only because of their excellent coordinating ability, but also of their large conjugated system and good accepter-donor system to form π-π interactions and hydrogen bonding interactions. Based on those factors, a number of coordination complexes have been prepared from zero-dimensional molecules or one-dimensional chains, generating extended two-dimensional layers or three-dimensional network supramolecular structures through π-π interactions and hydrogen bonding interactions[13, 14]. So, we selected 1,10-phenanthroline derivative, 2-(2-fluoro-6-fluorophenyl)-1*H*-imidazo[4,5-*f*][1,10]phenanthroline (L), as a N-donor chelating ligand and two carboxylate ligands as organic linkers, yielding two coordination complexes, namely [Mn(L)$_2$(DNSA)] (**1**) and [Co(L)(1,4-bdc)]$_n$ (**2**).

Received 10 June 2020; accepted 7 August 2020 (**CCDC 2017284 and 2017285**)

① Supported by the National Natural Science Foundation of China (No. 21805110)

① Corresponding author. Majoring in coordination chemistry. E-mail: wangxiuyanjlnu2004@163.com

2 EXPERIMENTAL

2. 1 Generals

The commercially available reagents were used without further purification. Elemental analysis was measured on a Perkin-Elmer 240 CHN elemental analyzer. The powder X-ray diffractions (PXRD) were measured on a Rigaku Dmax 2000 X-ray diffractometer with graphite-monochromatized Cu*Kα* radiation. The emission spectra were measured on a Renishaw inVia Raman Microscope. Thermal stability experiment was performed on a TG SDT2960 thermal analyzer under a nitrogen atmosphere.

2. 2 Synthesis of [Mn(L)$_2$(DNSA)] (1)

A mixture of H_2DNSA (0.30 mmol), $MnSO_4$ (0.30 mmol) and L (0.25 mmol) was dissolved in 12 mL water. When the pH value of the mixture was adjusted to ca. 7.5 with KOH, the solution was put into a 25-mL Teflon-lined Parr and heated in an autoclave at 150 ℃ for 4 days, obtaining yellow crystals of **1** in 31% yield based on L. Anal. Calcd. for $C_{45}H_{22}Cl_2F_2MnN_{10}O_7$ (%): C, 55.23; H, 2.27; N, 14.31. Found (%): C, 55.09; H, 2.23; N, 14.19.

2. 3 Synthesis of [Co(L)(1,4-bdc)]$_n$ (2)

The pH value of a mixture of 1,4-H_2bdc (0.30 mmol), $Co(NO_3)_2{\cdot}6H_2O$ (0.10 mmol) and L (0.05 mmol) in 10 mL water distilled water was adjusted to 5.7 with KOH. The resultant solution was heated at 185 ℃ in a 25-mL Teflon-lined stainless-steel autoclave for 4 days, resulting in brown crystals of **2** with the yield of 42% based on L. Anal. Calcd. for $C_{27}H_{14}ClCoFN_4O_4$ (%): C, 56.71; H, 2.47; N, 9.80. Found (%): C, 56.43; H, 2.41; N, 9.72.

2. 4 X-ray structure determination

A crystal of **1** suitable for X-ray diffraction was chosen and mounted on a Bruker P4 diffractometer equipped with graphite-monochromatized Mo*Kα* (λ = 0.71073 Å) radiation by using an ω scan method at 293(2) K. And a crystal of **2** was selected for data collection performed on a Rigaku RAXIS-RAPID CCD detector diffractometer equipped with graphite-monochromatic Mo*Kα* radiation (λ = 0.71073 Å) with an ω-ϕ scan mode at 293(2) K. The crystal structures were solved by direct methods with SIR2014 (Burla et al., 2014)[15] and refined with SHELXL2018/3 (Sheldrick, 2015)[16] by full-matrix least-squares techniques on F^2. The non-hydrogen atoms of the complex were refined with anisotropic temperature parameters. All H atoms were positioned geometrically (C–H = 0.93 Å) and refined as riding with U_{iso}(H) = 1.2U_{eq}(carrier).

3 RESULTS AND DISCUSSION

3. 1 Description of the crystal structure

Selected bond lengths and bond angles of **1** and **2** are given in Table 1, and hydrogen bond lengths and bond angles of **1** in Table 2. The asymmetric unit of **1** consists of one Mn(II) atom, two L ligands and one DNSA anion (Fig. 1). Each Mn(II) atom is six-coordinated by two oxygen atoms (O(1) and O(2)) from one DNSA anion, and four nitrogen atoms (N(1), N(2), N(5) and N(6) are from two L ligands in a distorted octahedral coordination sphere. The atoms N(1), N(2), N(5) and O(1) constitute the basal plane of the octahedron, while N(6) and O(2) are located at the axial positions. The Mn–O bond lengths range from 2.100(2) to 2.118(2) Å, and the Mn–N distances vary from 2.256(2) to 2.303(2) Å. The carboxylate group of DNSA anion shows a η^1:η^0 monodentate mode, whereas each DNSA anion chelates one Mn(II) atom in a bidentate mode. The adjacent [Mn(L)$_2$(DNSA)] molecules form a bimolecular structure through N–H···O (N(3)–H(3A)···O(2)^{ii}, N(3)–H(3A)···O(3)^{ii}, symmetric code: ^{ii} *x*–1, *y*, *z*–1, as shown in Table 2) hydrogen-bonding interactions (Fig. 2). Furthermore, the bimolecular structures are linked into a two-dimensional supramolecular layer structure by N–H···N (N(7)–H(7A)···N(4)^{v}, symmetric code: ^{v} *x*–1/2, –*y*+1/2, *z*+1/2, as illustrated in Table 2) hydrogen-bonding interactions between the adjacent bimolecular structures (Fig. 2).

Table 1. Selected Bond Lengths (Å) and Bond Angles (°) for 1 and 2

1					
Bond	Dist.	Bond	Dist.	Bond	Dist.
Mn(1)–N(1)	2.273(2)	Mn(1)–N(5)	2.278(2)	Mn(1)–O(1)	2.100(2)
Mn(1)–N(2)	2.303(2)	Mn(1)–N(6)	2.256(2)	Mn(1)–O(2)	2.118(2)
Angle	(°)	Angle	(°)	Angle	(°)
O(1)–Mn(1)–O(2)	81.91(7)	N(6)–Mn(1)–N(1)	107.66(8)	O(1)–Mn(1)–N(2)	90.03(8)
O(1)–Mn(1)–N(6)	90.68(7)	O(1)–Mn(1)–N(5)	107.28(8)	O(2)–Mn(1)–N(2)	108.05(8)
O(2)–Mn(1)–N(6)	157.26(8)	O(2)–Mn(1)–N(5)	88.80(8)	N(6)–Mn(1)–N(2)	93.35(8)

To be continued

O(1)–Mn(1)–N(1)	154.86(8)	N(6)–Mn(1)–N(5)	72.85(8)	N(1)–Mn(1)–N(2)	72.28(7)
O(2)–Mn(1)–N(1)	86.70(8)	N(1)–Mn(1)–N(5)	94.75(8)	N(5)–Mn(1)–N(2)	157.61(8)
2					
Bond	Dist.	Bond	Dist.	Bond	Dist.
N(1)–Co(1)	2.134(2)	N(2)–Co(1)	2.147(2)	O(1)–Co(1)	2.362(2)
O(2)–Co(1)	2.1231(18)	O(3)–Co(1)	2.0481(18)	O(4)–Co(1)^{iii}	2.0304(18)
Angle	(°)	Angle	(°)	Angle	(°)
O(4)^{iii}–Co(1)–O(3)	89.82(8)	O(4)^{iii}–Co(1)–O(2)	96.64(7)	O(3)–Co(1)–O(2)	101.94(7)
O(4)^{iii}–Co(1)–N(1)	121.30(8)	O(3)–Co(1)–N(1)	101.66(8)	O(2)–Co(1)–N(1)	134.87(7)
O(4)^{iii}–Co(1)–N(2)	86.11(8)	O(3)–Co(1)–N(2)	173.73(8)	O(2)–Co(1)–N(2)	83.29(8)
N(1)–Co(1)–N(2)	76.52(8)	O(4)^{iii}–Co(1)–O(1)	154.25(7)	O(3)–Co(1)–O(1)	91.90(7)
O(2)–Co(1)–O(1)	57.89(7)	N(1)–Co(1)–O(1)	83.45(7)	N(2)–Co(1)–O(1)	93.84(8)

Symmetry transformation used to generate the equivalent atoms:

[2] (i) $-x+1, y, -z+1/2$; (ii) $-x, -y+1, -z+1$; (iii) $-x, y, -z+1/2$

Table 2. Hydrogen Bond Lengths (Å) and Bond Angles (°) for 1

Crystal	D–H···A	d(D–H)	d(H···A)	d(D···A)	∠DHA
	N(3)–H(3A)···O(2)^{ii}	0.86	2.62	3.219(3)	127
1	N(3)–H(3A)···O(3)^{ii}	0.86	1.87	2.731(3)	175
	N(7)–H(7A)···N(4)^{v}	0.86	2.23	3.054(3)	160

Symmetry transformation: [1] (i) $x-1/2, -y+1/2, z-1/2$; (ii) $-x+1, -y, -z+1$; (iii) $-x+1/2, y-1/2, -z+3/2$; (iv) $-x+1/2, y+1/2, -z+1/2$; (v) $x-1/2, -y+1/2, z+1/2$

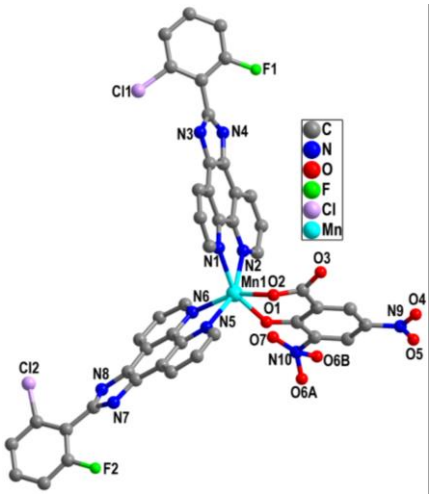

Fig. 1. View of the molecular structure of 1

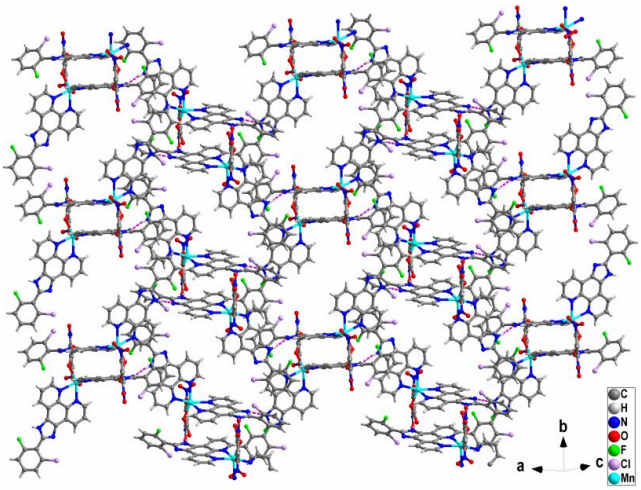

Fig. 2. View of the layer structure of 1 formed by hydrogen-bonding interactions (N–H ··O and N–H ··N)

As can be observed in Fig. 3, there are one Co(II) atom, one L ligand, and two halves of 1,4-bdc anions in the asymmetric unit of **2**. The 1,4-bdc anion resides on an inversion center. Each Co(II) atom is six-coordinated by two nitrogen atoms from one L ligand (Co(1)–N(1) = 2.134(2), Co(1)–N(2) = 2.147(2) Å), and four carboxylate oxygen atoms from three different 1,4-bdc anions (Co(1)–O(1) = 2.362(2), Co(1)–O(2) = 2.1231(18) Å, Co(1)–O(3) = 2.0481(18), Co(1)–O(4)^{iii} = 2.0304(18) Å, symmetric code: ^{iii} –*x*, *y*, –*z*+1/2). In particular, the two 1,4-bdc anions show different coordination modes (Fig. 3). For convenience, the 1,4-bdc anions containing the oxygen atoms labeled O(1) and O(3) are designated 1,4-bdc1 and 1,4-bdc2, respectively. Each carboxylate group of 1,4-bdc2 bridges two Co(II) atoms in a bis-bridging mode, whereas each carboxylate group of 1,4-bdc1 anion chelates one Co(II) atom in a bis-chelating mode to yield a dimer. The distance between the Co(II) atoms in the dimer is about 10.879 Å. Most interestingly, the binuclear units are bridged by the backbones of 1,4-bdc2 ligands to form a chain structure (Fig. 4) and are further connected by the 1,4-bdc2 ligands in bis-chelating modes to give rise to a layer structure (Fig. 4). The L ligands are attached to both sides of the layer structures, which allow the formation of π-π stacking between the two pyridine rings of the L ligands with the centroid-to-centroid distance of 3.764(2) Å and face-to-face distance of 3.387(1) Å, and the dihedral angle between the two planes is *ca*. 0.0(1)^{o} (Two pyridine rings are composed of N(1)/C(1) ~ C(5) and N(1)^{iv}/C(1)^{iv}~C(5)^{iv}, respectively; symmetry code: ^{iv} –*x* + 1/2, –*y* + 1/2, –*z* + 1) (Fig. 6). These π-π stacking interactions linked the adjacent layers into a 3D supramolecular architecture (Fig. 4).

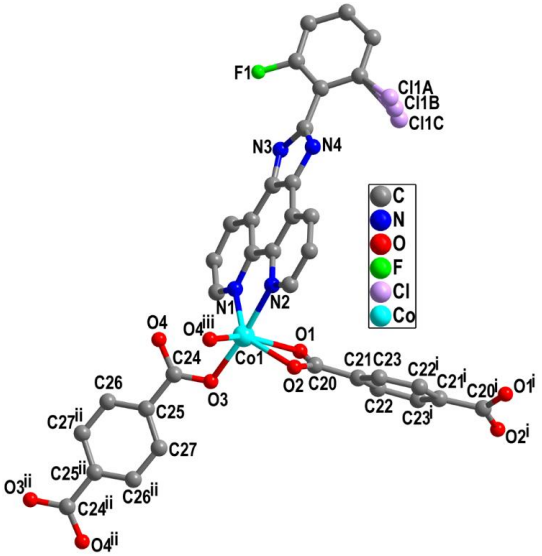

Fig. 3. Coordination environment of 2 (Symmetric codes: (i) –*x* + 1, *y*, –*z* + 1/2; (ii) –*x*, –*y* + 1, –*z* + 1; (iii) –*x*, *y*, –*z* + 1/2)

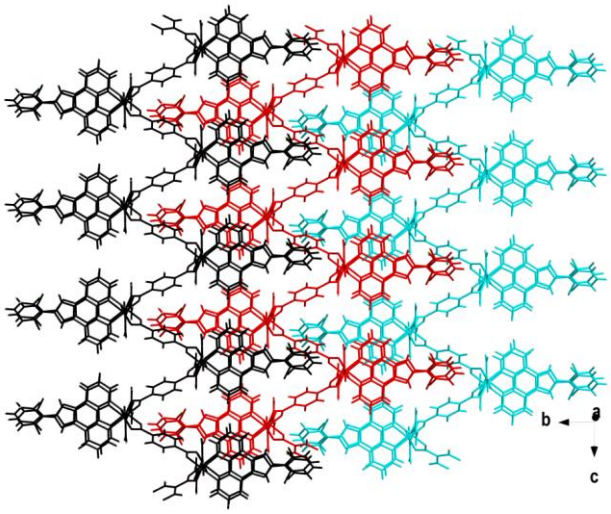

Fig. 4. Three-dimensional supramolecular architecture of the title complex constructed by π-π interactions

3. 2 PXRD patterns and UV-vis absorption spectrum

The powder X-ray diffraction (PXRD) patterns for complexes **1** and **2** were recorded at room temperature to confirm their phase purity (Fig. 5). The experimental PXRD patterns of **1** and **2** well correspond to the simulated ones of **1** and **2**, respectively, indicating the synthesized bulk materials and the measured single crystals are the same. The UV-vis absorption spectra of **1** were registered from the crystalline state at r. t. (Fig. 6). The energy bands of **1** from 200 to 560 nm can be assigned as metal-to-ligand charge-transfer (MLCT) transitions[17]. The above analysis is consistent with the crystal structure determination.

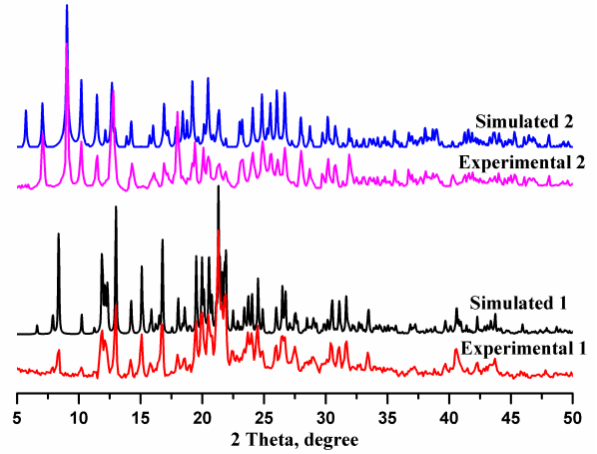

Fig. 5. Experimental and simulated PXRD patterns of 1 and 2

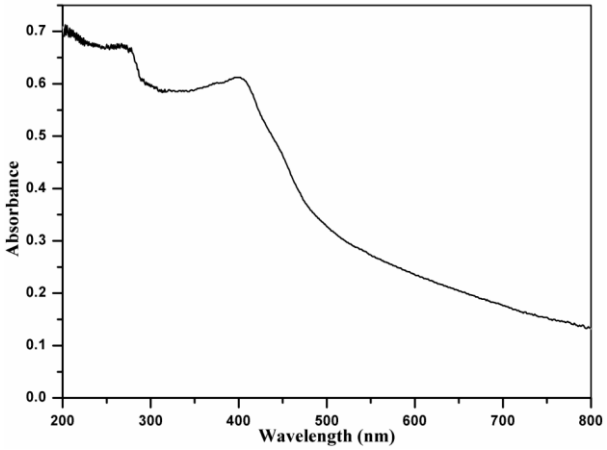

Fig. 6. UV-vis absorption spectrum of 1

3. 3 Luminescent properties

The luminescent properties of the free organic ligands and complex **1** have been studied in the solid state at room temperature (Fig. 7). The main emission peaks of H_2DNSA and L are located at about 548 (λ_{ex} = 325 nm) and 404 nm (λ_{ex} = 325 nm), respectively, which may be attributed to $\pi^* \rightarrow n$ or $\pi^* \rightarrow \pi$ transition[18]. Complex **1** shows an emission band at 545 nm (λ_{ex} = 325 nm). This emission is similar to that of H_2DNSA (λ_{em} = 545 nm). Therefore, the emission of **1** should originate from the H_2DNSA ligand.

3. 4 Thermogravimetric analysis

The stabilities of **1** and **2** were evaluated by thermogravimetric analysis (TGA). As depicted in Fig. 8, the TGA curve of **1** shows two main steps of weight loss. The first step of 21.4% from 202 to 310 ℃ corresponds to the release of the organic group $C_7H_2N_2O_6$ of DNSA anions (calcd. 21.5%), and the second step of 71.2% in the range of 317～572 ℃ to the elimination of L ligands (calcd.: 71.3%). The anhydrous complex **2** begins to decompose at 227 ℃ and ends above 632 ℃. The weight loss is attributed to both L ligands and the organic group $C_8H_4O_3$ of 1,4-bdc anions (obsd. 86.8%, calcd. 86.9%). However, it is difficult to determine this weight loss accurately as these processes are overlapped with the weight loss due to the dissociation of organic fractions.

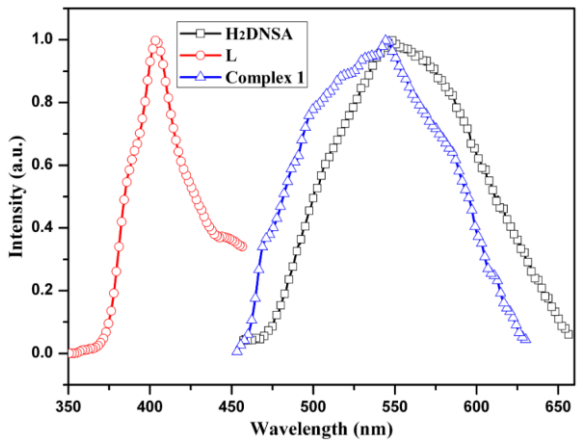

Fig. 7. Solid state emission spectra of 1,2,3-H_2DNSA, L and 1 at room temperature

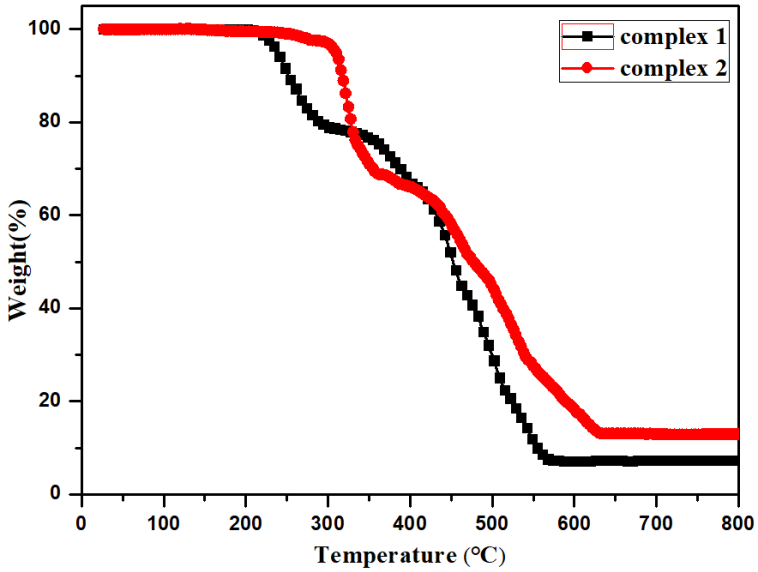

Fig. 8. TGA curves of complexes 1 and 2

4 CONCLUSION

Two new coordination complexes, $[Mn(L)_2(DNSA)]$ (**1**) and $[Co(L)(1,4\text{-bdc})]_n$ (**2**), have been successfully synthesized by the reaction of two transition metal ions, different aromatic carboxylic ligands and 2-(2-fluoro-6-fluorophenyl)-1H-imidazo[4,5-f][1,10]phenanthroline (L) with different architectures under hydrothermal conditions. The difference of the structures indicates that carboxylic ligands and metal cations play important roles in the formation of complexes. **1** shows weak emission in the solid state at room temperature. The thermal behaviors of **1** and **2** have been studied. We believe that more metal complexes containing L ligand with interesting structures and physical properties will be synthesized in the future.

REFERENCES

(1) Eddaoudi, M.; Moler, D. B.; Li, H.; Chen, B.; Reineke, T. M.; O'Keeffe, M.; Yaghi, O. M. Modular chemistry: secondary building units as a basis for the design of highly porous and robust metal-organic carboxylate frameworks. *Acc. Chem. Res.* **2001**, 34, 319–330.

(2) Yoshii, Y.; Sakai, K.; Hoshino, N.; Takeda, T.; Noro, S.; Nakamura, T.; Akutagawa, T. Crystal-to-crystal structural transformation of hydrogen-bonding molecular crystals of (imidazolium)(3-hydroxy-2-quinoxalinecarboxylate) through H_2O adsorption-desorption. *CrystEngComm.* **2015**, 17, 5962–5969.

(3) Kong, Z. G.; Guo, S. N.; Zhao, X. Y.; An, X. An unusual 2D → 3D polythreading framework based on (4)-c sql networks with arms: synthesis, structure and luminescence. *Mendeleev Commun.* **2016**, 26, 52–53.

(4) Zheng, B. S.; Luo, X.; Wang, Z. X.; Zhang, S. W.; Yun, R. R.; Huang, L.; Zeng, W. J.; Liu, W. L. An unprecedented water stable acylamide-functionalized metal-organic framework for highly efficient CH_4/CO_2 gas storage/separation and acid-base cooperative catalytic activity. *Inorg. Chem. Front.* **2018**, 5, 2355–2363.

(5) Sebastian, H.; Andreas, S.; Shobhna, K.; Roland, W.; Roland, A. F. Zinc-1,4-benzenedicarboxylate-bipyridineframeworks-linker functionalization impacts network topology during solvothermal synthesis. *J. Mater. Chem.* **2012**, 22, 909–918.

(6) Han, X.; Xu, Y. X.; Yang, J.; Xu, X.; Li, C. P.; Ma, J. F. Metal-assembled, resorcin[4]arene-based molecular trimer for efficient removal of toxic dichromate pollutants and knoevenagel condensation Reaction. *ACS Appl. Mater. Inter.* **2019**, 11, 15591–15597.

(7) Rubio-Martinez, M.; Avci-Camur, C.; Thornton, A. W.; Imaz, I.; Maspoch, D.; Hill, M. R. New synthetic routes towards MOF production at scale. *Chem. Soc. Rev.* **2017**, 46, 3453–3480.

(8) Martin, B. D.; Suzanne, M. N.; Stuart, R. B. Variable length ligands: a new class of bridging ligands for supramolecular chemistry and crystal engineering. *Chem. Commun.* **2009**, 37, 5579–5581.

(9) Wang, X. Y.; Li, G. T.; Wang, H.; Song, Y.; Liu, D. X; Xu, Z. L. Crystal structure, thermal behavior and luminescence of a new copper coordination polymer constructed with 4-(carboxymethoxy)-benzoic acid. *Chin. J. Struct. Chem.* **2019**, 38, 629–634.

(10) Mala, N.; Pramendra, K. S. Chemistry and applications of organotin(IV) complexes of Schiff bases. *Dalton Trans.* **2011**, 40, 7077–7121.

(11) Lin, Z. J.; Lü, J.; Hong, M. C.; Cao, R. Metal-organic frameworks based on flexible ligands (FL-MOFs): structures and applications. *Chem. Soc. Rev*. **2014**, 43, 5867–5895.

(12) Ferey, G. Microporous solids: from organically templated inorganic skeletons to hybrid frameworks···ecumenism in chemistry. *Chem. Mater*. **2001**, 13, 3084–3098.

(13) Wang, X. Y.; He, Y.; Zhao, L. N.; Kong, Z. G. An unusual 2D → 3D polythreading framework based on a long 1,10-phenanthroline derivative ligand. *Inorg. Chem. Commun*. **2011**, 14, 1186–1189.

(14) Kong, Z. G.; Han, Q.; Zhang, L.; Liu, D. X.; Hu, B.; Wang, X. Y. A new Cd(II) coordination polymer constructed by 1,10-phenanthroline derivative:syntheses, structure, physical properties and theoretical calculation. *Chin. J. Struct. Chem.* **2019**, 38, 2141–2147.

(15) Burla, M. C.; Caliandro, R.; Carrozzini, B.; Cascarano, G. L.; Cuocci, C.; Giacovazzo, C.; Mallamo, M.; Mazzone, A.; Polidori, G. Crystal structure determination and refinement via SIR2014. *J. Appl. Cryst*. **2015**, 48, 306–309.

(16) Sheldrick, G. M. Crystal structure refinement with SHELXL. *Acta Cryst.* **2015**, C71, 3–8.

(17) Chen, X. M.; Liu, G. F. Double-stranded helices and molecular zippers assembled from single-stranded coordination polymers directed by supramolecular interactions. *Chem. Eur. J.* **2002**, 8, 4811–4817.

(18) Zhang, S. H.; Feng, C. Microwave-assisted synthesis, crystal structure and fluorescence of novel coordination complexes with Schiff base ligands. *J. Mol. Struct.* **2010**, 997, 62–66.